THERMOACOUSTIC ENGINES AND REFRIGERATORS

On the heels of basic research, commercial developers are harnessing acoustic processes in gases to make reliable, inexpensive engines and cooling devices with no moving parts and a significant fraction of Carnot's efficiency.

Gregory W. Swift

We ordinarily think of a sound wave in a gas as consisting of coupled pressure and displacement oscillations. However, temperature oscillations always accompany the pressure changes. The combination of all these oscillations, and their interaction with solid boundaries, produces a rich variety of "thermoacoustic" effects. Although these effects as they occur in everyday life are too small to be noticed, one can harness extremely loud sound waves in acoustically sealed chambers to produce powerful heat engines, heat pumps and refrigerators. Whereas typical engines and refrigerators have crankshaft-coupled pistons or rotating turbines, thermoacoustic engines and refrigerators have at most a single flexing moving part (as in a loudspeaker) with no sliding seals. Thermoacoustic devices may be of practical use where simplicity, reliability or low cost is more important than the highest efficiency (although one cannot say much more about their cost-competitiveness at this early stage).

The basics: Thermoacoustic engines

A thermoacoustic engine converts some heat from a high-temperature heat source into acoustic power, rejecting waste heat to a low-temperature heat sink. The heat-driven electrical generator shown in figure 1 illustrates the basic principle of operation. The overall view, shown at the top of figure 1a, is reminiscent of the appearance of a heat engine in many introductory thermodynamics texts: The apparatus absorbs heat per unit time Q_h from a heat source at high temperature T_h, rejects heat per unit time Q_c to a heat sink at low temperature T_c and produces acoustic power W. The first law of thermodynamics tells us that $W + Q_c = Q_h$; the second law shows that the efficiency W/Q_h is bounded above by the Carnot efficiency $(T_h - T_c)/T_h$. (I will use Q and W for heat power and acoustic power, and q and w for the corresponding energies.)

One of the most important scales in a thermoacoustic device is the length of its resonator, which (together with the gas sound speed) determines the operating frequency, just as the length of an organ pipe determines its pitch. This length typically falls between 10 cm and 10 m. In figure 1a, with both ends of the resonator closed, the lowest resonant mode is that which fits a half-wavelength standing wave in the resonator, with displacement nodes and pressure antinodes at the ends, as shown in the lower portion of figure 1. The heat-exchange elements—a hot heat exchanger, a cold heat exchanger and a "stack" between them—are located where both oscillating pressure and oscillating gas displacement are nonzero. Each of the two heat exchangers is typically a set of copper fins, as open to gas flow as possible (like a car radiator), and is thermally anchored to its reservoir by metallic heat conduction or circulating fluids. The stack is simply a well-spaced stack of solid plates with high heat capacity, also quite open to gas flow, supporting the smooth temperature profile between the two heat exchangers as shown at the bottom of figure 1a. Most of the "parallel plate" stacks constructed so far have in fact been spirally wound, a low-cost configuration.

To understand in some detail the conversion of heat to acoustic power by this simple structure, consider the magnified view of part of the stack in figure 1b, which shows a typical parcel of gas at four instants of time during one cycle of the acoustic wave. The standing wave carries the parcel left and right, compressing and expanding it, with phasing such that it is at its most compressed state when at its farthest left position, and its most expanded state at its farthest right position. In typical thermoacoustic engines and refrigerators the amplitude of the pressure oscillation is 3–10% of the mean pressure, and the displacement amplitude is a similar percentage of the length of a plate in the stack.

The presence of an externally imposed temperature gradient in the stack adds a new feature to what would otherwise be a simple acoustic oscillation: oscillatory heat transfer between the parcel of gas and the stack. (To simplify this discussion, I will neglect the adiabatic temperature oscillations that accompany the pressure oscillations.) When the parcel is at its leftmost position, heat flows from the relatively hot stack plate to the parcel, expanding it; when the parcel is at its rightmost position, heat flows from it to the relatively cool stack plate, contracting the parcel. The parcel does net work on its surroundings, because the expansion takes place at the high-pressure phase of the cycle and the contraction at the low-pressure phase, as shown in figure 1c.

(Readers with Internet access are encouraged to view our computer animations of this process and of thermoacoustic refrigeration as described below. The thermoacoustics home page is at http://rott.esa.lanl.gov/; select "educational

GREGORY SWIFT *works in the condensed matter and thermal physics group at Los Alamos National Laboratory, in New Mexico.*

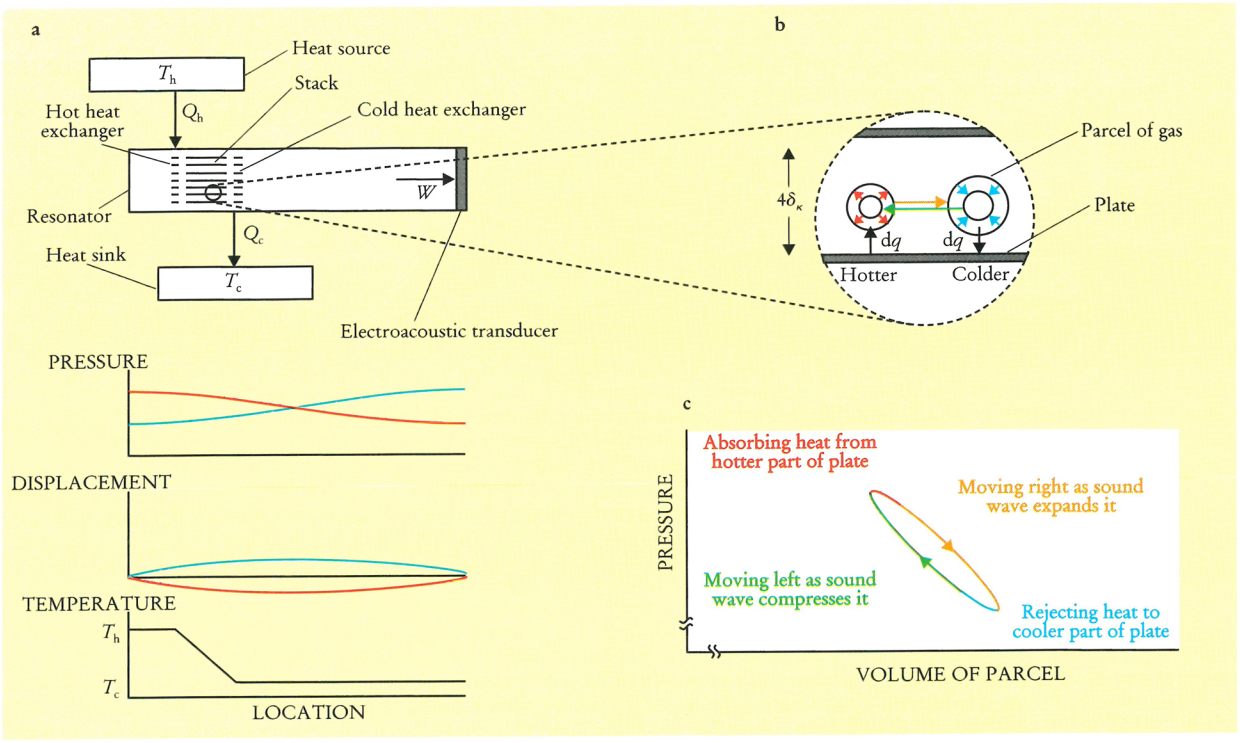

SIMPLE THERMOACOUSTIC ENGINE. **a:** Heat exchangers and a stack in a half-wavelength acoustic resonator convert some of the heat power Q_h from a thermal reservoir at temperature T_h into acoustic power W, rejecting waste heat power Q_c to another reservoir at T_c. The acoustic power is delivered to an electroacoustic transducer, which converts it to electricity. Plots below show gas pressure, gas displacement in the horizontal direction and average temperature as functions of location in the resonator. Pressure and displacement are each shown when the gas is at the leftmost extreme of its displacement (red), with density and pressure highest at the left end of the resonator and lowest at the right end, and 180° later in the cycle (blue). **b:** Magnified view of part of the stack shows a typical parcel of gas (greatly exaggerated in size) as it oscillates in position, pressure and temperature, exchanging heat dq with the nearby plates of the stack. Plates are separated by about four thermal penetration depths δ_κ. **c:** Pressure–volume (p–V) diagram for the parcel of gas shows how it does net work $\delta w = \oint p\, dV$ on its surroundings. **FIGURE 1**

demonstrations." For DOS-based computers, the executable file FANCY.EXE and text file FANCY.TXT can be downloaded.)

The net work that the parcel does on its surroundings is delivered in each cycle of the acoustic oscillation. The parcel and all others like it within the stack deliver acoustic power W to the standing wave; the standing wave delivers it in turn to the electroacoustic transducer. Each parcel absorbs a little heat from one location in the stack and deposits a little heat farther to the right, at a cooler location in the stack. With respect to heat, all the parcels act like members of a bucket brigade, with the overall effect being absorption of Q_h at the hot heat exchanger and rejection of Q_c at the cold heat exchanger.

A second important scale in a thermoacoustic engine is the separation between plates in the stack, which determines the nature of thermal contact between the plate and the typical parcel of gas. Imperfect thermal contact is needed to accomplish the cycle shown in figure 1, because it is desirable to have good thermal contact when the parcel is stationary or nearly so, but poor thermal contact while it is moving. Detailed analysis shows that a spacing between plates of about four thermal penetration depths $\delta_\kappa = \sqrt{\kappa/\pi f \rho c_p}$ is best, where κ is the thermal conductivity of the gas, ρ is its density, c_p its isobaric specific heat per unit mass and f the frequency of the acoustic oscillation; δ_κ is roughly the distance heat can diffuse through the gas during a time $1/\pi f$. In today's thermoacoustic systems, δ_κ is typically a fraction of a millimeter.

Heat-driven acoustic oscillators such as that shown in figure 1 have been known for over a century. The earliest and simplest, known as the Sondhauss tube, was discovered accidentally by European glassblowers; a later example, the Taconis oscillator, is well known today to users of liquid helium. In each of these early thermoacoustic engines, the resonator itself was only several δ_κ in diameter, and its walls also served the functions of stack and heat exchangers. The use of an explicit stack (with multiple parallel passages) and heat exchangers in larger-diameter resonators to increase overall power began with Robert L. Carter in the 1960s.[1]

Although progress toward a theoretical understanding of these phenomena began with Lord Rayleigh 120 years ago, a quantitatively accurate theory of thermoacoustics was not developed until the 1970s, through the efforts of Nicholas Rott and coworkers.[2] This theory is based on a low-amplitude linearization of the Navier–Stokes, continuity and energy equations with sinusoidal oscillations of all variables. It is remarkable that such qualitatively simple classical phenomena went without a quantitatively accurate explanation until late in this century.

The basics: Thermoacoustic refrigerators

Another chapter in the development of thermoacoustics began at Los Alamos National Laboratory in the early

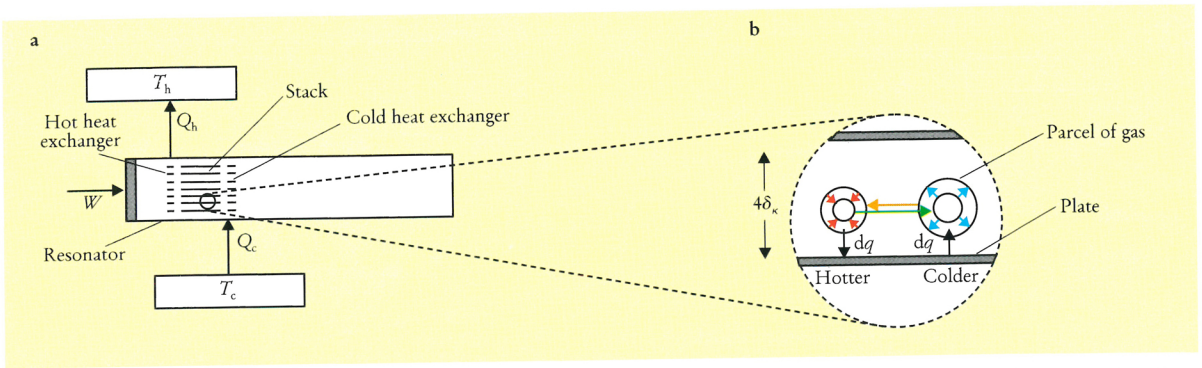

SIMPLE THERMOACOUSTIC REFRIGERATOR. **a:** Electroacoustic transducer at the left end delivers acoustic power W to the resonator, producing refrigeration Q_c at low temperature T_c and rejecting waste heat power Q_h to a heat sink at T_h. As in figure 1, this is a half-wavelength device with a pressure node at the midpoint of the resonator. The temperature gradient in the refrigerator's stack is much less steep than that in the stack for the engine shown in figure 1. **b:** Magnified view of part of the stack shows a typical parcel of gas as it moves heat dq up the temperature gradient. Here $\oint p\,dV < 0$, so the pressure–volume cycle analogous to figure 1c goes counterclockwise, and the parcel absorbs work from its surroundings. **FIGURE 2**

1980s with the invention of thermoacoustic refrigeration.[3] The basic principle of operation, illustrated in figure 2, is very similar to that of thermoacoustic engines, but here the temperature gradient in the stack is much lower. As the gas oscillates along the stack, it experiences changes in temperature. Much of the gas's temperature change comes from adiabatic compression and expansion of the gas by the acoustic pressure, and the rest is a consequence of heat transfer with the stack. At the leftmost position of the parcel of gas shown in figure 2b, it rejects heat to the stack, because its temperature was raised above the local stack temperature by adiabatic compression caused by the standing wave. Similarly, at its rightmost position, the parcel absorbs heat from the stack, because adiabatic expansion has brought its temperature below the local stack temperature. Thus the parcel of gas moves a little heat from right to left along the stack, up the temperature gradient, during each cycle of the acoustic wave.

All the other parcels in the stack behave similarly, so that the overall effect, again as in a bucket brigade, is the net transport of heat from the cold heat exchanger to the hot heat exchanger, with Q_c absorbed at T_c and Q_h rejected at T_h. The parcel absorbs acoustic work from the standing wave, because the thermal expansion of the parcel of gas occurs during the low-pressure phase of the acoustic wave and the thermal contraction during the high-pressure phase. The resulting acoustic power W absorbed by all the parcels in the stack can be supplied by a loudspeaker, a thermoacoustic engine or other means. The first law of thermodynamics once again determines that $W + Q_c = Q_h$; the second law shows that the relevant efficiency, known as the coefficient of performance, is bounded above by the Carnot coefficient $T_c/(T_h - T_c)$.

The steepness of the temperature gradient in the stack determines whether a thermoacoustic device is a refrigerator (which has work done on it) or an engine (which does work). In an engine, with a steep temperature gradient as shown in figure 1, the gas parcel finds itself cooler than the local stack temperature after its adiabatic compression during displacement to the left, so it absorbs heat from the stack at high pressure and expands. In contrast, in a refrigerator, with a shallow gradient, the gas parcel finds itself warmer than the local stack temperature after its adiabatic compression during displacement to the left, so it rejects heat to the higher-temperature part of the stack and contracts.

Figure 3a shows schematically the first efficient thermoacoustic refrigerator,[4] designed, built and studied by Tom Hofler. It illustrates several features of many of today's thermoacoustic devices. The resonator had a slightly complicated geometry, which maintained the desired frequency, pressure amplitude and displacement amplitude at the stack while reducing the total length to much less than half the wavelength. This geometry also reduced viscous and thermal losses on the resonator walls and suppressed the harmonic content so that the sound wave remained purely sinusoidal in time. The pressure antinode is at the driver piston, and the pressure node is at the widening neck near the sphere, so this is essentially a quarter-wavelength apparatus, even though the spatial dependence of the pressure is not exactly a cosine. High-pressure helium gas was used: High pressure increases the power per unit volume of apparatus, and helium, having the highest sound speed and thermal conductivity of the inert gases, further increases the power density and allows spacings within the stack and heat exchangers to be as large as possible, for ease of fabrication. The loudspeaker-like driver was located at a pressure antinode of the standing wave, so that the acoustic power was delivered with high force and small displacement, easing engineering difficulties associated with the flexing portion of the driver. This location also placed it next to the hot heat exchanger, where heat generated in the driver could be removed most efficiently.

Figure 3b shows some of the data obtained with this refrigerator, which reached a T_c of –70 °C and had a cooling power of several watts with acoustic pressure amplitudes of 3% of the mean pressure. The curves in the figure were calculated using publicly available software[5] based on the theory developed by Rott and are in reasonable agreement with the data. The calculations have no adjustable parameters; they simply use the geometry of the apparatus and the properties of helium gas.

Commercial developments

Attempts to develop practical devices based on thermoacoustics began just a few years ago, throughout the US and on four other continents. This surge of interest was due to the interaction of several factors: the new "tech transfer" emphasis at government laboratories; the engineering development of some thermoacoustic refrigerators at the Naval Postgraduate School in Monterey, California,

under the enthusiastic leadership of Steve Garrett; the crisis in the refrigeration industry caused by the destruction of stratospheric ozone by chlorofluorocarbons; and the marriage of thermoacoustic engines with orifice pulse-tube refrigerators (discussed below). To illustrate the breadth of applications under way, I have chosen four examples from among the corporate-sponsored thermoacoustics projects that I know of.

The thermoacoustic refrigerator shown in figure 4a is a prototype for a food refrigerator. Built at CSIR (formerly called the Council for Scientific and Industrial Research) in the Republic of South Africa with corporate support, it is a direct descendant of a thermoacoustic refrigerator[6] that was originally intended for preserving blood and urine samples on the space shuttle. It is a symmetrical, essentially half-wavelength device driven by modified loudspeakers on both ends, with two stacks, each with two heat exchangers. The pressure node is at the center of the bottom section. Use of two stacks maximizes cooling power for a given resonator size, all other things being equal. For compactness, the fiberglass resonator is formed in a "U" shape, with little effect on the acoustics. Cooling power (typically 100 W) and temperatures are appropriate for residential food refrigeration in most of the world. (American refrigerators are larger than most and hence require about twice as much cooling power.)

Scientists at Ford Motor Company built the thermoacoustic refrigerator depicted on the cover of this issue. The driver is at the displacement maximum of the quarter-wavelength standing wave (instead of at the pressure maximum as in the refrigerators of figures 3a and 4a). Thus in this refrigerator acoustic power is delivered with small pressure and large volumetric displacement, accomplished by using a large area in the driver. The driver's losses flow to the cold heat exchanger, but this is a minor problem if the driver is efficient and T_c is not too far below T_h. Water inlet and outlet tubes (gray in the diagram), essentially serving as the hot and cold thermal reservoirs, are clearly visible at the heat exchangers. This device operates at 10 bars with either helium driven at 430 Hz or a mixture of 80% helium—20% argon driven at 260 Hz.

At Tektronix Corporation in Beaverton, Oregon, researchers are developing a system for cooling electronics to cryogenic temperatures. A thermoacoustic engine drives an orifice pulse-tube refrigerator,[7] which is related to both Stirling and thermoacoustic refrigerators. The system thus constitutes a heat-driven cryogenic refrigerator having no moving parts; it has cooled to 150 K. It has a half-wavelength resonator with resistively heated thermoacoustic engines near both ends. In a sidebranch, 500 W of acoustic power from these engines is delivered to the pulse-tube refrigerator.

The largest thermoacoustic engine to date, under construction at Cryenco Inc in Denver, Colorado, will also drive a pulse-tube refrigerator. The heat source for the engine will be natural gas combustion. Intended for industrial and commercial liquefaction of natural gas it will measure 12 meters long, and will use two ½-meter-diameter spiral stacks (figure 4b) to produce 40 kW of acoustic power at 40 Hz in 30-bar helium gas. The device should be completed this year.

Power and efficiency

The power of thermoacoustic devices is roughly proportional to $p_{avg}Aa(p_{osc}/p_{avg})^2$, where p_{avg} is the average pressure, A the cross-sectional area of the stack, a the sound

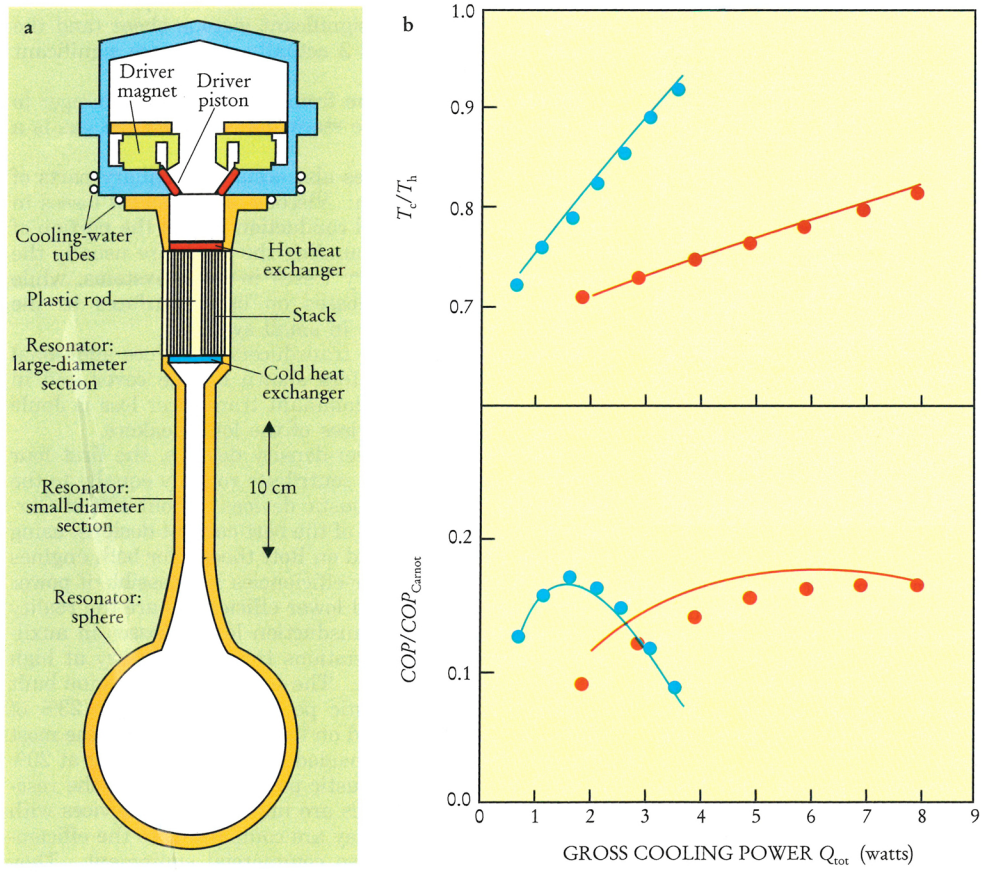

FIRST EFFICIENT THERMOACOUSTIC REFRIGERATOR (a) and some of its performance parameters (b) as measured[4] (data points) and calculated[5] (curves) for operation with 500-Hz pressure oscillations in 10-bar helium gas, and with T_h = 300 K. Blue circles are data for 1.5% pressure oscillations; red circles, 3%. The gross cooling power Q_{tot} includes the deliberately applied load plus some small parasitic loads such as heat leak from room temperature. The coefficient of performance (*COP*) equals Q_{tot}/W, with W the acoustic power delivered to the resonator. **FIGURE 3**

a

b

TWO COMMERCIALLY INTERESTING thermoacoustic systems. **a:** Half-wavelength refrigerator with two stacks driven by two loudspeakers was built at CSIR in South Africa. It operates at 120 Hz with 15-bar neon. The heat exchangers are located where the water lines connect to the green resonator body. (Courtesy of Peter Bland, Quadrant.) **b:** One of the two spiral stacks for the largest thermoacoustic engine to date, being built by Cryenco Inc. (Courtesy of John Wollan, Cryenco.) **FIGURE 4**

speed of the gas and p_{osc} the amplitude of the oscillatory pressure. Helium (with high sound speed) is often used, typically at a pressure above 10 bars. In the examples cited in the previous section, p_{osc}/p_{avg} values range from 0.03 to 0.10, chosen as design compromises between the high power density achieved at high amplitude and the high confidence in the quantitative accuracy of Rott-based calculations at low amplitude.

The efficiency of thermoacoustic devices falls below Carnot's efficiency because of five major sources of irreversibility—"inherent," viscous, conduction, auxiliary and transduction losses:

▷ Inherent loss arises from the heat transfer to and from each parcel of gas in the stack as shown in figures 1 and 2: Whenever heat dq is transferred across a nonzero temperature difference δT, the entropy of the universe increases[8] by $dq\ \delta T/T^2$. This irreversibility is unavoidable in the thermoacoustic process, relying as it does on imperfect thermal contact for the correct phasing between pressure oscillations and thermal expansion–contraction.

▷ Viscous loss in the stack occurs because work must be done to overcome viscous shear forces as the gas oscillates between the plates. The viscous penetration depth $\delta_\mu = \sqrt{\mu/\pi f\rho}$ (where μ is viscosity) is comparable to the thermal penetration depth, so most of the space between the plates experiences significant viscous shear (and the parcels in figures 1 and 2 actually experience significant shape distortions).

▷ Simple heat conduction from the hot heat exchanger to the cold one through the stack material and the gas is a further loss.

▷ These first three losses also occur in auxiliary parts of a thermoacoustic system: Viscous and inherent losses in the heat exchangers and conduction loss in the portion of the resonator case surrounding the stack are usually the most important auxiliary losses in large systems, while viscous and inherent losses on other surfaces in the resonator are important in small systems.

▷ Electroacoustic power transducers introduce additional loss. For the refrigerators shown on the cover and in figures 3a and 4a, the dominant transducer loss is Joule heating in the copper wires of the loudspeakers.

For many high-power-density designs, the first four sources of irreversibility contribute roughly equally to the inefficiency of thermoacoustic devices. About 40% of Carnot's efficiency is typical of the best current designs, using computer modeling based on Rott theory, for both engines and refrigerators; higher efficiencies are possible if power density is sacrificed, and lower efficiencies are the reality when electroacoustic transduction losses, losses in auxiliary equipment and deviations from Rott theory at high amplitudes are included. The most efficient engine built to date delivered acoustic power to its load at 23% of Carnot's efficiency (based on total heater power); the most efficient refrigerator[9] provided gross cooling power at 20% of Carnot (based on acoustic power delivered to the resonator). These efficiencies are impressive for devices with no moving parts, and they are comparable to the efficiencies of small, inexpensive commercial equipment. They

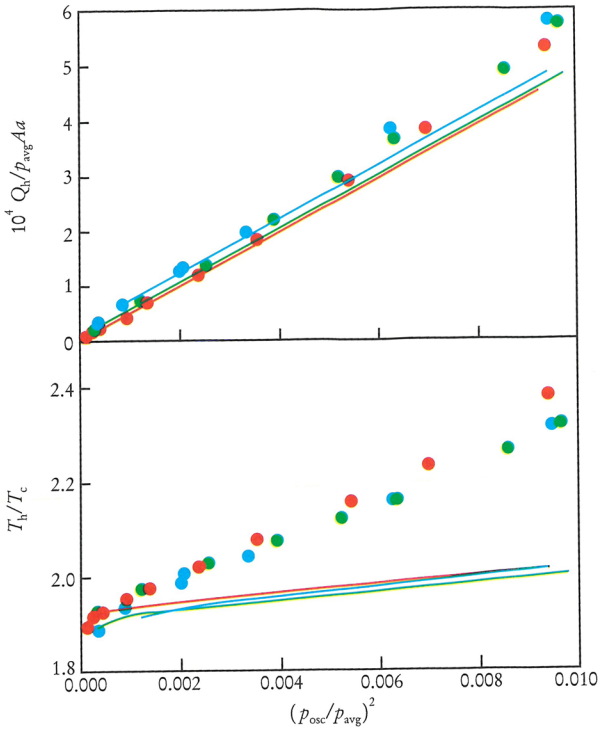

RECENT MEASUREMENTS AND CALCULATIONS for a thermoacoustic engine similar to that shown in figure 1, but with no transducer. The heater power Q_h, hot temperature T_h and oscillating pressure amplitude p_{osc} are all normalized, but note the different vertical scales. Circles are measurements from ref. 16; lines are calculations done using ref. 5. Red is for helium at 0.96 megapascals; green, neon at 0.70 MPa; blue, argon at 0.359 MPa. These pressures were chosen to make the thermal penetration depth δ_κ equal to 0.22 mm at the cold end (T_c) in all cases. **FIGURE 5**

fall far short of the efficiencies of well-engineered, expensive steam turbines or large-scale vapor-compression refrigeration equipment, for which over 80% of Carnot's efficiency has been achieved.

If future inventions and improvements to basic understanding can improve the efficiency or raise the power density of thermoacoustic engines and refrigerators without sacrificing their simplicity, they will find more widespread use. One way to increase efficiency, first demonstrated by Hofler,[4] is to use a mixture of helium and a heavier inert gas as the working substance. The Prandtl number $\sigma = \mu c_p/\kappa = \delta_\mu^2/\delta_\kappa^2$ is a dimensionless measure of the ratio of viscous to thermal effects in fluids; lower Prandtl numbers give higher efficiencies in thermoacoustics. Kinetic theory predicts $\sigma = \frac{2}{3}$ for hard-sphere monatomic gases, and indeed real monatomic gases have values very close to this. (For instance, helium at room temperature has $\sigma = 0.68$.) Fortunately mixtures of a heavy and a light monatomic gas have Prandtl numbers significantly lower than $\frac{2}{3}$. The thermoacoustic refrigerator intended for the space shuttle that was mentioned above[6] used 89% helium and 11% xenon, with $\sigma = 0.27$, to achieve its 20% efficiency, compared with 17% efficiency for the similar apparatus shown in figure 3 when optimized for pure helium gas. However, with a sound speed less than half that of pure helium, the gas mixture reduced the power density.

Beyond the basics

In the US our understanding of thermoacoustics is advancing beyond the foundations established by Rott, thanks to physicists at many universities and national laboratories.

Rott and his collaborators considered two geometries for thermoacoustic processes: parallel-plate channels (most commonly used, as we have discussed above) and circular channels. Wondering if some geometries might be better than others, W. Patrick Arnott, Henry Bass and Richard Raspet[10] at the University of Mississippi added rectangular and triangular channels, established a common formalism for all channel geometries and concluded that parallel-plate channels are the most efficient. The reason is subtle: Viscous losses occur mostly at and near channel walls, *within* a characteristic distance equal to the viscous penetration depth δ_μ, while the desirable thermoacoustic effects portrayed in figures 1 and 2 occur mostly away from walls, at a characteristic distance equal to the thermal penetration depth δ_κ *from* them. Thus for the usual case of $\delta_\mu \approx \delta_\kappa$, extremely concave channels (imagine triangles) squeeze the desirable effects into a small fraction of the channel cross-sectional area in the center, leaving a relatively large area near the perimeter causing viscous loss. Capitalizing on this analysis, Ulrich Müller has proposed that the "channels" formed by the space in a two-dimensional array of parallel wires[11] (aligned along the direction of acoustic oscillation and spaced by a few δ_κ) would give even higher efficiency than parallel plates. Tapered channels[12] and modifications of the phase between pressure and velocity[13] are also being studied for improving efficiency.

The most promising route to higher power densities is increasing $(p_{osc}/p_{avg})^2$, but doing so will take us further from the range of small oscillations on which Rott theory and its current extensions are fundamentally based. Rott's assumptions include the following:

▷ a gas displacement amplitude much smaller than the length of the stack and other components

▷ a Reynolds number of the oscillations small enough to avoid turbulence

▷ $p_{osc} \ll p_{avg}$.

Extensions beyond each of these limitations have begun.

At the Naval Postgraduate School, Anthony Atchley and his colleagues[14] have undertaken high-amplitude experiments on the simplest possible thermoacoustic device, a short stack with no heat exchangers in a loudspeaker-driven resonator. Their data extend into the large-gas-displacement regime, with amplitudes approaching the length of the stack.

A growing body of literature is establishing the characteristics of several regimes of turbulent oscillatory flow[15] at high Reynolds numbers, although as yet there are no fundamental studies of heat transfer under these conditions.

A similitude study has shown[16] how to organize and correlate experimental data in the high-amplitude range, allowing meaningful experimental studies of scale models of thermoacoustic devices reminiscent of wind-tunnel studies of model aircraft.

Researchers at several institutions, including Johns Hopkins University and Los Alamos and Livermore National Laboratories, are beginning numerical and analytical studies that seek to illuminate other features of high-amplitude thermoacoustics.

Figure 5 illustrates the amplitude dependence of the accuracy of our current understanding of thermoacoustic phenomena. The data shown as points were taken from a no-load thermoacoustic engine.[16] The plots can be interpreted as displaying the required heater power Q_h and temperature T_h at the hot heat exchanger for maintaining steady oscillations at a given pressure amplitude p_{osc}. Three monatomic gases were used, with average pressures selected to make δ_κ the same for all three cases, ensuring similarity; the data for all three gases do indeed fall along the same curves. The lines are the results of calculations based on Rott's theory, the dimensions of the apparatus and the properties of the gases. The calculations agree well with the measurements in the limit of small p_{osc}, as expected from the assumptions in the theory. However, as p_{osc}/p_{avg} approaches 0.1, the measurements deviate significantly from calculations. The deviations are not surprising, in that they are of the same order as p_{osc}/p_{avg}, but they are disturbing from a practical point of view because both Q_h and T_h deviate in directions that decrease the efficiency.

The fundamentals of thermoacoustics at low amplitudes are reasonably well understood, and a few practical uses of thermoacoustics have been tentatively identified. Much study, engineering and especially invention remains to be done before these simple, elegant devices reach their full potential.

Most of the fundamental research on thermoacoustics in the US is supported by the Department of Energy and the Office of Naval Research. Most of the applied developments are supported privately but with important contributions from ARPA, DOE and the Navy. I am particularly grateful to DOE's Office of Basic Energy Sciences for its steady support of thermoacoustics research at Los Alamos. This article benefited from constructive criticism by Hank Bass, Steve Garrett and Tom Hofler.

References

1. K. T. Feldman, J. Sound Vib. **7**, 71 (1968).
2. N. Rott, Z. Angew. Math Phys. **20**, 230 (1969); **26**, 43 (1975). Reviewed by G. W. Swift, J. Acoust. Soc. Am. **84**, 1145 (1988).
3. J. C. Wheatley, T. J. Hofler, G. W. Swift, A. Migliori, J. Acoust. Soc. Am. **74**, 153 (1983).
4. T. J. Hofler, PhD dissertation, U. Calif., San Diego (1986). T. J. Hofler, in *Proc. 5th Int. Cryocoolers Conf.*, P. Lindquist, ed., Wright–Patterson Air Force Base, Ohio (1988), p. 93.
5. W. C. Ward, G. W. Swift, J. Acoust. Soc. Am. **95**, 3671 (1994). Fully tested software and users guide available from Energy Science and Technology Software Center, US Dept. of Energy, Oak Ridge, Tenn. For a beta-test version, contact ww@lanl.gov (Bill Ward) via Internet.
6. S. L. Garrett, D. K. Perkins, A. Gopinath, in *Heat Transfer 1994: Proc. 10th Int. Heat Transfer Conf.*, G. F. Hewitt, ed., Inst. Chem. Eng., Rugby, UK (1994), p. 375.
7. R. Radebaugh, Adv. Cryogenic Eng. **35**, 1191 (1990).
8. A. Bejan, *Entropy Generation Through Heat and Fluid Flow*, Wiley, New York (1982).
9. S. L. Garrett, J. A. Adeff, T. J. Hofler, J. Thermophys. Heat Transfer **7**, 595 (1993).
10. W. P. Arnott, H. E. Bass, R. Raspet, J. Acoust. Soc. Am. **90**, 3228 (1991).
11. U. A. Müller, US patent 4 625 517 (1986). G. W. Swift, R. M. Keolian, J. Acoust. Soc. Am. **94**, 941 (1993).
12. N. Rott, G. Zouzoulas, Z. Angew. Math. Phys. **27**, 197 (1976). U. A. Müller, PhD dissertation 7014, Eidgenössische Technische Hochschule, Zurich, Switzerland (1982).
13. R. Raspet, H. E. Bass, J. Kordomenos, J. Acoust. Soc. Am. **94**, 2232 (1993). P. H. Ceperley, J. Acoust. Soc. Am. **66**, 1508 (1979).
14. A. A. Atchley, T. J. Hofler, M. L. Muzzerall, M. D. Kite, C. Ao, J. Acoust. Soc. Am. **88**, 251 (1990).
15. R. Akhavan, R. D. Kamm, A. H. Shapiro, J. Fluid Mech. **225**, 395, 423 (1991).
16. J. R. Olson, G. W. Swift, J. Acoust. Soc. Am. **95**, 1405 (1994). ■